Simone Barcellona[1], Maria Stefania Carmeli[2,*], Gabrio Superti-Furga[3]

J. Electrical Systems 9-3 (2013): 290-300

Regular paper

Comparison between Matrix Converter and Indirect Matrix Converter

JES
Journal of Electrical Systems

Three-phase to three-phase power conversion with variable frequency and output voltage amplitude control can be realized with both matrix converter and indirect matrix converter configurations. Even if this two power converters have a different topology, the indirect configuration provides an equivalent circuit widely used to define matrix converter modulation strategies. The equivalence between the states of the two converters is well known but a discussion on indirect matrix converter relationships has never been deeply investigated. This paper discusses the equivalence between the two power converter configurations from a mathematical viewpoint, pointing out the intrinsic characteristics and potentialities of each of them.

Keywords: AC-AC conversion, matrix converter, indirect matrix converter, power converter topology, power electronics

1. Introduction

A three-phase/three-phase Matrix Converter (MC) consists of nine bidirectional switches (Fig. 1), that make it possible any output phase to be connected to any input one [1]-[4]. As any standard converter, a set of voltage-controlled ports are connected to a set of current-controlled ones by means of switches. The voltage-controlled ports are supported by capacitors, the current-controlled ones are supported by inductors.

On the other hand, Indirect Matrix Converter (IMC) (Fig. 2) comprises a three-phase Current Source Converter (CSC), used as controlled rectifier bridge, and a three-phase Voltage Source Converter (VSC), connected to a common dc bus without any storage element on the dc side. The different kinds of IMC proposed in literature (as Sparse IMC, Ultra Sparse IMC) [5]-[7] differ in the CSC topology, which mainly affects power flow direction.

The IMC offers similar features of MC but it also provides an equivalent circuit widely used to define MC control strategy. Indeed the control of MC is not an easy task to be realized. The decomposition into an equivalent IMC makes it possible to adopt well known control techniques over CSC and VSC components. As a matter of fact, the different control strategies for MC proposed in literature [3], [8]-[11] can be divided in two categories: direct modulation methods [12]-[16] and indirect modulation ones [17]-[20]. The latter uses the concept of fictitious dc link to control MC by means of a virtual IMC.

It is well-known the equivalence among the states of the two converters but some states of MC, known as rotating ones, cannot be realized by IMC because of the virtual two wires dc link connection. Hence in indirect modulation methods these rotating states cannot be used and often also in direct modulation ones are not considered [2]. In spite of a wide use of IMC approach to MC, the basic relationships of the IMC as a whole system are not yet completely exploited or discussed. The aim of this paper is to fill this gap. This paper discusses the equivalence between MC and IMC from a mathematical viewpoint, the intrinsic characteristic and potentiality of each configuration is pointed out.

The present paper is organized as follows. In Sect. 2 the consolidated relationships of MC are pointed out. In Sect. 3 novel basic equations for IMC are proposed. In Sect. 4-5 the

1 DEIB Dept. Politecnico di Milano, Milan, Italy
2* Corresponding author: M. S. Carmeli, Mechanical Engineering Dept, Politecnico di Milano, via La Masa 1, 20156 Milan. Italy, E-mail: stefania.carmeli@polimi.it
3 Politecnico di Milano, Milan, Italy. Retired

correspondences between IMC and MC relationships are discussed considering the switching states.

2. Matrix Converter

The relationships between input (subscript 1) and output (subscript 2) phase quantities (a, b, c) are shown in (1)-(3), where s_{ij} = 0,1 are primary Switching Functions (SF) of each ideal switch (Fig. 1).

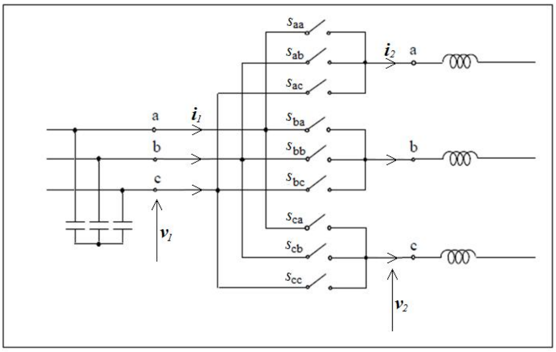

Fig. 1. Three-phase Matrix Converter

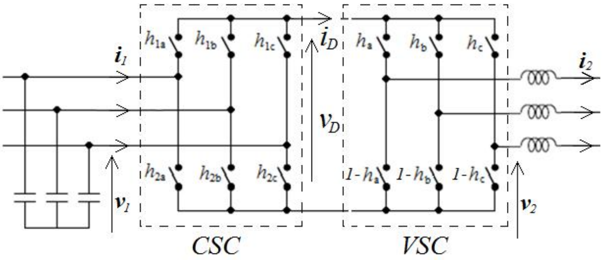

Fig. 2. Three-phase Indirect Matrix Converter

$$\begin{bmatrix} v_{2a} \\ v_{2b} \\ v_{2c} \end{bmatrix} = \begin{bmatrix} s_{aa} & s_{ab} & s_{ac} \\ s_{ba} & s_{bb} & s_{bc} \\ s_{ca} & s_{cb} & s_{cc} \end{bmatrix} \begin{bmatrix} v_{1a} \\ v_{1b} \\ v_{1c} \end{bmatrix} \quad (1)$$

$$\begin{bmatrix} i_{1a} \\ i_{1b} \\ i_{1c} \end{bmatrix} = \begin{bmatrix} s_{aa} & s_{ba} & s_{ca} \\ s_{ab} & s_{bb} & s_{cb} \\ s_{ac} & s_{bc} & s_{cc} \end{bmatrix} \begin{bmatrix} i_{2a} \\ i_{2b} \\ i_{2c} \end{bmatrix} \quad (2)$$

$$\begin{aligned} s_{aa} + s_{ab} + s_{ac} &= 1 \\ s_{ba} + s_{bb} + s_{bc} &= 1 \\ s_{ca} + s_{cb} + s_{cc} &= 1. \end{aligned} \quad (3)$$

In order to avoid short circuits between input phases and interruptions of the output currents, only one bidirectional switch for each output phase can be turned on. In particular the possible switching configurations are limited to 27 according to (3).

A wide use of space-vectors to represent three-phase three-wire system is proposed in what follows.

Let *a*, *b*, *c* be the subscripts of phase quantities. Applying the modified Clarke transformation to the instantaneous values, the space-vectors of voltage and current are defined

$$\boldsymbol{v} = \sqrt{2/3}\left(v_a + \boldsymbol{\alpha} v_b + \boldsymbol{\alpha}^2 v_c\right)$$
$$\boldsymbol{i} = \sqrt{2/3}\left(i_a + \boldsymbol{\alpha} i_b + \boldsymbol{\alpha}^2 i_c\right) \tag{4}$$

where $\boldsymbol{\alpha} = e^{j\frac{2\pi}{3}}$.

The instantaneous power associated to space-vectors (4) is $p = \mathrm{Re}(\boldsymbol{v}\boldsymbol{i}^*)$.

The instantaneous zero sequence components are not considered because they are not involved in the present paper.

Applying (4) to (1) and (2), after some mathematical manipulations, the following space-vector relationships between input-output quantities can be written

$$\boldsymbol{v}_2 = \boldsymbol{s}_i^* \boldsymbol{v}_1 + \boldsymbol{s}_d \boldsymbol{v}_1^* \tag{5}$$

$$\boldsymbol{i}_1 = \boldsymbol{s}_i \boldsymbol{i}_2 + \boldsymbol{s}_d \boldsymbol{i}_2^* \tag{6}$$

where

$$\boldsymbol{s}_d = \frac{1}{3}\left(\boldsymbol{s}_a + \boldsymbol{\alpha}\boldsymbol{s}_b + \boldsymbol{\alpha}^2 \boldsymbol{s}_c\right) \tag{7}$$

$$\boldsymbol{s}_i = \frac{1}{3}\left(\boldsymbol{s}_a + \boldsymbol{\alpha}^2 \boldsymbol{s}_b + \boldsymbol{\alpha}\boldsymbol{s}_c\right) \tag{8}$$

$$\boldsymbol{s}_a = s_{aa} + \boldsymbol{\alpha} s_{ab} + \boldsymbol{\alpha}^2 s_{ac}$$
$$\boldsymbol{s}_b = s_{ba} + \boldsymbol{\alpha} s_{bb} + \boldsymbol{\alpha}^2 s_{bc} \tag{9}$$
$$\boldsymbol{s}_c = s_{ca} + \boldsymbol{\alpha} s_{cb} + \boldsymbol{\alpha}^2 s_{cc}.$$

In this way, comprehensive and compact mathematical representation is adopted to study MC. Similar results (5), (6) have been firstly obtained in [9] and referenced in [11]. Voltage $\boldsymbol{v}_1$ and current $\boldsymbol{i}_2$ are state variables over the conservative elements and input variables for MC.

It can be recognize that (5)-(6) satisfy the input-output power balance. Because of this power condition, $\boldsymbol{v}_2$ and $\boldsymbol{i}_1$ cannot be controlled separately by (5)-(6), consequently the system has only three control freedom degrees.

From (7)-(9) and taking into account the constraints (3), 27 possible switching configurations can be obtained, as reported in Table 1. In particular we have: 3 nil configurations (1-3), 18 active fixed configurations (4-21) and 6 rotating active configurations (22-27).

In what follows the auxiliary indexes *s*, c_R s_R k_R δ_d, δ_i as assigned in Table 1, are used.

TABLE 1: SWITCHING CONFIGURATIONS

N°	c_R	s_R	k_R	s	δ_d	δ_i	Active Switches	Output Voltage	Input Current	s_d	s_i
1	-	-	-	0	-	-	$s_{aa} = s_{ba} = s_{ca} = 1$	$\boldsymbol{v}_2 = 0$	$\boldsymbol{i}_1 = 0$	0	0
2	-	-	-	0	-	-	$s_{ab} = s_{bb} = s_{cb} = 1$	$\boldsymbol{v}_2 = 0$	$\boldsymbol{i}_1 = 0$	0	0
3	-	-	-	0	-	-	$s_{ac} = s_{bc} = s_{cc} = 1$	$\boldsymbol{v}_2 = 0$	$\boldsymbol{i}_1 = 0$	0	0
4	0	-	-	1	0	0	$s_{aa} = s_{bb} = s_{cb} = 1$	$\boldsymbol{v}_2 = K_v v_{1ab}$	$\boldsymbol{i}_1 = j\boldsymbol{\alpha}^2 K_i i_{2a}$	$Ke^{-j\pi/6}$	$Ke^{-j\pi/6}$

5	0	-	-	1	3	3	$s_{ab}=s_{ba}=s_{ca}=1$	$\boldsymbol{v}_2=-K_v v_{1ab}$	$\boldsymbol{i}_1=-j\boldsymbol{\alpha}^2 K_i i_{2a}$	$Ke^{j5\pi/6}$	$Ke^{j5\pi/6}$
6	0	-	-	1	2	2	$s_{ab}=s_{bc}=s_{cc}=1$	$\boldsymbol{v}_2=K_v v_{1bc}$	$\boldsymbol{i}_1=jK_i i_{2a}$	$Ke^{j\pi/2}$	$Ke^{j\pi/2}$
7	0	-	-	1	5	5	$s_{ac}=s_{bb}=s_{cb}=1$	$\boldsymbol{v}_2=-K_v v_{1bc}$	$\boldsymbol{i}_1=-jK_i i_{2a}$	$Ke^{-j\pi/2}$	$Ke^{-j\pi/2}$
8	0	-	-	1	4	4	$s_{ac}=s_{ba}=s_{ca}=1$	$\boldsymbol{v}_2=K_v v_{1ca}$	$\boldsymbol{i}_1=-j\boldsymbol{\alpha} K_i i_{2a}$	$Ke^{-j5\pi 6}$	$Ke^{-j5\pi 6}$
9	0	-	-	1	1	1	$s_{aa}=s_{bc}=s_{cc}=1$	$\boldsymbol{v}_2=-K_v v_{1ca}$	$\boldsymbol{i}_1=j\boldsymbol{\alpha} K_i i_{2a}$	$Ke^{j\pi/6}$	$Ke^{j\pi/6}$
10	0	-	-	1	2	4	$s_{ab}=s_{ba}=s_{cb}=1$	$\boldsymbol{v}_2=K_v\boldsymbol{\alpha} v_{1ab}$	$\boldsymbol{i}_1=j\boldsymbol{\alpha}^2 K_i i_{2b}$	$Ke^{j\pi/2}$	$Ke^{-j5\pi 6}$
11	0	-	-	1	5	1	$s_{aa}=s_{bb}=s_{ca}=1$	$\boldsymbol{v}_2=-K_v\boldsymbol{\alpha} v_{1ab}$	$\boldsymbol{i}_1=-j\boldsymbol{\alpha}^2 K_i i_{2b}$	$Ke^{-j\pi/2}$	$Ke^{j\pi/6}$
12	0	-	-	1	4	0	$s_{ac}=s_{bb}=s_{cc}=1$	$\boldsymbol{v}_2=K_v\boldsymbol{\alpha} v_{1bc}$	$\boldsymbol{i}_1=jK_i i_{2b}$	$Ke^{-j5\pi 6}$	$Ke^{-j\pi/6}$
13	0	-	-	1	1	3	$s_{ab}=s_{bc}=s_{cb}=1$	$\boldsymbol{v}_2=-K_v\boldsymbol{\alpha} v_{1bc}$	$\boldsymbol{i}_1=-jK_i i_{2b}$	$Ke^{j\pi/6}$	$Ke^{j5\pi/6}$
14	0	-	-	1	0	2	$s_{aa}=s_{bc}=s_{ca}=1$	$\boldsymbol{v}_2=K_v\boldsymbol{\alpha} v_{1ca}$	$\boldsymbol{i}_1=-j\boldsymbol{\alpha} K_i i_{2b}$	$Ke^{-j\pi/6}$	$Ke^{j\pi/2}$
15	0	-	-	1	3	5	$s_{ac}=s_{ba}=s_{cc}=1$	$\boldsymbol{v}_2=-K_v\boldsymbol{\alpha} v_{1ca}$	$\boldsymbol{i}_1=j\boldsymbol{\alpha} K_i i_{2b}$	$Ke^{j5\pi/6}$	$Ke^{-j\pi/2}$
16	0	-	-	1	4	2	$s_{ab}=s_{bb}=s_{ca}=1$	$\boldsymbol{v}_2=K_v\boldsymbol{\alpha}^2 v_{1ab}$	$\boldsymbol{i}_1=j\boldsymbol{\alpha}^2 K_i i_{2c}$	$Ke^{-j5\pi 6}$	$Ke^{j\pi/2}$
17	0	-	-	1	1	5	$s_{aa}=s_{ba}=s_{cb}=1$	$\boldsymbol{v}_2=-K_v\boldsymbol{\alpha}^2 v_{1ab}$	$\boldsymbol{i}_1=-j\boldsymbol{\alpha}^2 K_i i_{2c}$	$Ke^{j\pi/6}$	$Ke^{-j\pi/2}$
18	0	-	-	1	0	4	$s_{ac}=s_{bc}=s_{cb}=1$	$\boldsymbol{v}_2=K_v\boldsymbol{\alpha}^2 v_{1bc}$	$\boldsymbol{i}_1=jK_i i_{2c}$	$Ke^{-j\pi/6}$	$Ke^{-j5\pi 6}$
19	0	-	-	1	3	1	$s_{ab}=s_{bb}=s_{cc}=1$	$\boldsymbol{v}_2=-K_v\boldsymbol{\alpha}^2 v_{1bc}$	$\boldsymbol{i}_1=-jK_i i_{2c}$	$Ke^{j5\pi/6}$	$Ke^{j\pi/6}$
20	0	-	-	1	2	0	$s_{aa}=s_{ba}=s_{cc}=1$	$\boldsymbol{v}_2=K_v\boldsymbol{\alpha}^2 v_{1ca}$	$\boldsymbol{i}_1=-j\boldsymbol{\alpha} K_i i_{2c}$	$Ke^{j\pi/2}$	$Ke^{-j\pi/6}$
21	0	-	-	1	5	3	$s_{ac}=s_{bc}=s_{ca}=1$	$\boldsymbol{v}_2=-K_v\boldsymbol{\alpha}^2 v_{1ca}$	$\boldsymbol{i}_1=j\boldsymbol{\alpha} K_i i_{2c}$	$Ke^{-j\pi/2}$	$Ke^{j5\pi/6}$
22	1	1	0	1	-	-	$s_{aa}=s_{bb}=s_{cc}=1$	$\boldsymbol{v}_2=\boldsymbol{v}_1$	$\boldsymbol{i}_1=\boldsymbol{i}_2$	0	1
23	1	0	0	1	-	-	$s_{aa}=s_{bc}=s_{cb}=1$	$\boldsymbol{v}_2=\boldsymbol{v}_1^*$	$\boldsymbol{i}_1=\boldsymbol{i}_2^*$	1	0
24	1	0	1	1	-	-	$s_{ab}=s_{ba}=s_{cc}=1$	$\boldsymbol{v}_2=\boldsymbol{\alpha}\boldsymbol{v}_1^*$	$\boldsymbol{i}_1=\boldsymbol{\alpha}\boldsymbol{i}_2^*$	$\boldsymbol{\alpha}$	0
25	1	1	1	1	-	-	$s_{ab}=s_{bc}=s_{ca}=1$	$\boldsymbol{v}_2=\boldsymbol{\alpha}^2\boldsymbol{v}_1$	$\boldsymbol{i}_1=\boldsymbol{\alpha}\boldsymbol{i}_2$	0	$\boldsymbol{\alpha}$
26	1	0	2	1	-	-	$s_{ac}=s_{bb}=s_{ca}=1$	$\boldsymbol{v}_2=\boldsymbol{\alpha}^2\boldsymbol{v}_1^*$	$\boldsymbol{i}_1=\boldsymbol{\alpha}^2\boldsymbol{i}_2^*$	$\boldsymbol{\alpha}^2$	0
27	1	1	2	1	-	-	$s_{ac}=s_{ba}=s_{cb}=1$	$\boldsymbol{v}_2=\boldsymbol{\alpha}\boldsymbol{v}_1$	$\boldsymbol{i}_1=\boldsymbol{\alpha}^2\boldsymbol{i}_2$	0	$\boldsymbol{\alpha}^2$

$K=1/\sqrt{3}$ K_v $\sqrt{2/3}$ K_i $\sqrt{2}$

From Table 1 $\boldsymbol{s}_d$ and $\boldsymbol{s}_i$ can be reorganized in two groups of terms: rotating terms and fixed ones.

$$\boldsymbol{s}_d = c_R \boldsymbol{s}_{dR} + \left(1-c_R\right)\boldsymbol{s}_{dF} \tag{10}$$

$$\boldsymbol{s}_i = c_R \boldsymbol{s}_{iR} + \left(1-c_R\right)\boldsymbol{s}_{iF}. \tag{11}$$

Rotating terms are

$$\boldsymbol{s}_{dR} = s\left(1-s_R\right)e^{j\left(k_R\frac{2}{3}\pi\right)} \tag{12}$$

$$\boldsymbol{s}_{iR} = s s_R e^{j\left(k_R\frac{2}{3}\pi\right)} \tag{13}$$

And fixed terms are

$$\boldsymbol{s}_{dF} = s\left[\frac{1}{\sqrt{3}} e^{j\frac{\pi}{3}\left(\delta_d - \frac{1}{2}\right)}\right] \tag{14}$$

$$\boldsymbol{s}_{iF} = s\left[\frac{1}{\sqrt{3}} e^{j\frac{\pi}{3}\left(\delta_i - \frac{1}{2}\right)}\right]. \tag{15}$$

According to Table 1, the states of $\boldsymbol{s}_d$ and $\boldsymbol{s}_i$ can be represented in the complex plane as shown in Fig. 3.

It must be observed from Table 1 and indexes in Fig. 3 that $\boldsymbol{s}_d$ and $\boldsymbol{s}_i$ are not independent of each other and cannot be freely assigned.

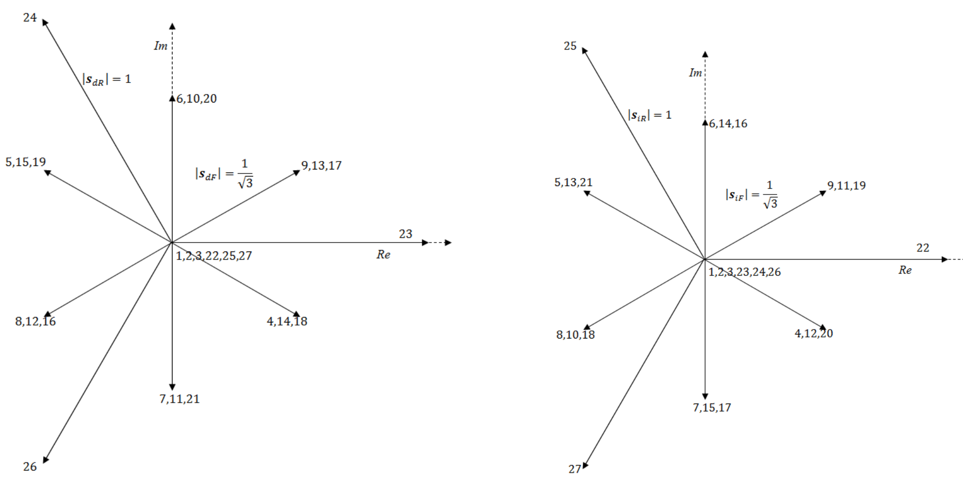

a) $\boldsymbol{s}_d$ b) $\boldsymbol{s}_i$

Fig. 3. Swithing states according to Table 1

3. Indirect Matrix Converter

The mathematical relationships of IMC can be obtained starting from the relationships of the CSC and of the VSC and taking into account the coupling of the dc link common to both, as pointed out in the following subsections.

3.1. CSC stage

The CSC has the voltage $\boldsymbol{v}_1$ as ac impressed port and the current i_D as dc impressed port, as shown in Fig. 2. Only one switch for each row must be turned on to avoid short circuits at ac side and open circuit at dc one. Hence 9 switching configurations are possible: 3 nil and 6 fixed active ones. These configurations can be reorganized in the complex SF $\boldsymbol{h}_i$ of CSC $(h_{ij} = 0,1)$

$$\boldsymbol{h}_i = \sqrt{\frac{2}{3}}\left[h_{1a} - h_{2a} + \boldsymbol{\alpha}(h_{1b} - h_{2b}) + \boldsymbol{\alpha}^2(h_{1c} - h_{2c})\right] \tag{16}$$

with

$h_{1a} + h_{1b} + h_{1c} = 1$, $h_{2a} + h_{2b} + h_{2c} = 1$.

The (16) can be rewritten in polar form as

$$\boldsymbol{h}_i = \sqrt{2} n_i e^{j\frac{\pi}{3}(k_i - \frac{1}{2})}$$
$$n_i = 0,1; \quad k_i = 0,1,2,3,4,5 \tag{17}$$

depicted in the hexagon of Fig. 4.

From Fig. 2 and (16) and considering the power balance, the constitutive relationships in Clark domain of CSC are

$$v_D = \text{Re}(\boldsymbol{h}_i^* \boldsymbol{v}_1) \tag{18}$$

$$\boldsymbol{i}_1 = \boldsymbol{h}_i i_D. \tag{19}$$

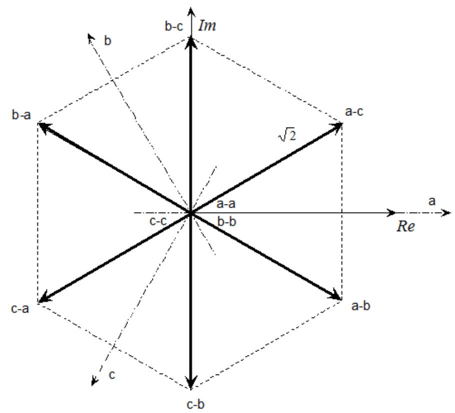

Fig. 4. Complex Switching Function of CSC. Indexes *a, b, c* refer to phases (upper and lower) involved in the indicated switching state.

3.2. VSC stage

The VSC has the current $\boldsymbol{i}_2$ as ac impressed port and the voltage v_D as dc impressed port, as shown in Fig. 2. Only one switch for each column must be turned on to avoid short circuits at dc side and open circuits at ac one. Consequently, 8 combinations are possible: 2 nil and 6 fixed active ones. These configurations can be reorganized in the complex SF $\boldsymbol{h}_v$ of VSC ($h_j = 0,1$)

$$\boldsymbol{h}_v = \sqrt{\frac{2}{3}} \left(h_a + \boldsymbol{\alpha} h_b + \boldsymbol{\alpha}^2 h_c \right). \tag{20}$$

The (20) can be rewritten in polar form as

$$\boldsymbol{h}_v = \sqrt{\frac{2}{3}} n_v e^{j\frac{\pi}{3}k_v}$$
$$n_v = 0,1; k_v = 0,1,2,3,4,5 \tag{21}$$

depicted in the hexagon of Fig. 5.

From (20) and considering the power balance, the constitutive relationships in Clark domain of VSC are

$$\boldsymbol{v}_2 = \boldsymbol{h}_v v_D \tag{22}$$

$$i_D = \text{Re}\left(\boldsymbol{h}_v^* \boldsymbol{i}_2 \right). \tag{23}$$

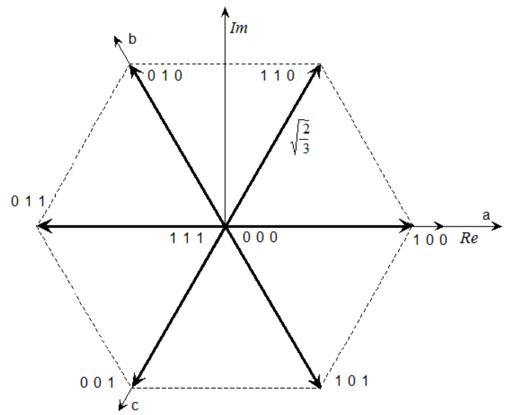

Fig. 5. Complex Switching Function of VSC. Indexes 0, 1 refer to on/off state of phases *a, b, c*.

3.3. Indirect MC

The equations of IMC are obtained connecting CSC with VSC through the common dc link. From a mathematical point of view let us consider eqs. (18)-(19) with (22)-(23). Then (24) and (25) hold:

$$\boldsymbol{v}_2 = \boldsymbol{h}_v \operatorname{Re}\left(\boldsymbol{h}_i^* \boldsymbol{v}_1\right) \tag{24}$$

$$\boldsymbol{i}_1 = \boldsymbol{h}_i \operatorname{Re}\left(\boldsymbol{h}_v^* \boldsymbol{i}_2\right). \tag{25}$$

The (24) and (25) can be rewritten as (26) and (27):

$$\boldsymbol{v}_2 = \frac{\boldsymbol{h}_v \boldsymbol{h}_i^*}{2} \boldsymbol{v}_1 + \frac{\boldsymbol{h}_v \boldsymbol{h}_i}{2} \boldsymbol{v}_1^* \tag{26}$$

$$\boldsymbol{i}_1 = \frac{\boldsymbol{h}_v^* \boldsymbol{h}_i}{2} \boldsymbol{i}_2 + \frac{\boldsymbol{h}_v \boldsymbol{h}_i}{2} \boldsymbol{i}_2^*. \tag{27}$$

Taking into account (17) and (21) we have:

$$\begin{aligned} \frac{\boldsymbol{h}_v \boldsymbol{h}_i}{2} &= \frac{1}{\sqrt{3}} n e^{j\frac{\pi}{3}(k_i + k_v - \frac{1}{2})} \\ \frac{\boldsymbol{h}_v^* \boldsymbol{h}_i}{2} &= \frac{1}{\sqrt{3}} n e^{j\frac{\pi}{3}(k_i - k_v - \frac{1}{2})} \\ n &= n_v n_i = 0,1. \end{aligned} \tag{28}$$

Eqs. (26) and (27) depend on the product of two SFs $\boldsymbol{h}_v$ and $\boldsymbol{h}_i$. Since $\boldsymbol{h}_v$ has 8 switching configurations and $\boldsymbol{h}_i$ has 9 ones, then 72 total possible combinations are deduced: 36 nil ones (either or both $\boldsymbol{h}_v$, $\boldsymbol{h}_i$ are nil), and 36 fixed active ones. Of these 36 fixed active configurations just 18 are different at the three-phase ports because the others 18 give the same output voltage and input current space vectors but with opposite DC link polarity. The values of these 18 active combinations are the same of the 18 fixed active configurations of MC, as will be shown.

4. From IMC to MC

Eqs. (26) and (27) have the same form of (5) and (6) and (28) are similar to (14) and (15).

In order to establish a relation between SFs (28) of the IMC and (10), (11) of the MC, the following equivalences are forced

$$\frac{\boldsymbol{h}_v \boldsymbol{h}_i}{2} = \boldsymbol{s}_d \tag{29}$$

$$\frac{\boldsymbol{h}_v^* \boldsymbol{h}_i}{2} = \boldsymbol{s}_i \tag{30}$$

under the conditions in (12)-(15)

$$\begin{aligned} &\boldsymbol{s}_{dR} = \boldsymbol{s}_{iR} = 0 \\ &\delta_d = mod(k_i + k_v, 6) \\ &\delta_i = mod(k_i - k_v, 6) \\ &s = n. \end{aligned} \tag{31}$$

It should be pointed out that (28) reproduces the Fig. 3 a) and b), but limited to an hexagon vertexes and nil values, whereas the larger states of unity amplitude are not reproduced, as they are associated to the rotating states of MC. From (31) the correlations between $\boldsymbol{s}_d$ and $\boldsymbol{s}_i$ are evidenced. As a matter of fact, each couple of k_v and k_i generates $\boldsymbol{s}_d$ and $\boldsymbol{s}_i$ correlated each other. Hence eqs. (29), (30), (31) express the equivalence between IMC and MC fixed states. As outstanding result, it can be stated that IMC and MC are equivalent only considering the 18 fixed active configurations and 3 nil ones of MC.

The correspondence between the switching states of the IMC and the ones of MC can be stated from (29), (30) by taking into account (7)-(9) and (16), (20). After some mathematical manipulations, relations (32) are obtained

$$\begin{aligned} s_{aa} &= h_a h_{1a} + h_{2a} - h_{2a} h_a \\ s_{ab} &= h_a h_{1b} + h_{2b} - h_{2b} h_a \\ s_{ac} &= h_a h_{1c} + h_{2c} - h_{2c} h_a \\ s_{ba} &= h_b h_{1a} + h_{2a} - h_{2a} h_b \\ s_{bb} &= h_b h_{1b} + h_{2b} - h_{2b} h_b \\ s_{bc} &= h_b h_{1c} + h_{2c} - h_{2c} h_b \\ s_{ca} &= h_c h_{1a} + h_{2a} - h_{2a} h_c \\ s_{cb} &= h_c h_{1b} + h_{2b} - h_{2b} h_c \\ s_{cc} &= h_c h_{1c} + h_{2c} - h_{2c} h_c . \end{aligned} \tag{32}$$

The MC has 6 rotating active configurations more than IMC. As a matter of fact rotating configurations could be realized connecting each output phase to a different input one, but this is not allowed in IMC because of the two terminals interposed dc link. From mathematical point-of-view, in IMC when $\boldsymbol{s}_d$ is zero also $\boldsymbol{s}_i$ is zero, as both depend on the same terms $\boldsymbol{h}_v$ and $\boldsymbol{h}_i$ in (29)-(30), whereas only one of them has to be zero (v. Tab. I) to obtain a rotating configuration.

5. Averaged Relations

Let us deal with control criteria and operation limits over instantaneous values averaged with respect to the ripple switching frequency. Such average process is correct under the so-called frequency separation condition, which is verified if the spectra of the entire converter input variables are bounded to a frequency much smaller than the converter switching one. The averaged values are indicated with upper case.

Let us consider the voltages and currents in polar form:

$$\boldsymbol{V}_1 = V_1 e^{j\vartheta_1} \tag{33}$$

$$\boldsymbol{V}_2 = V_2 e^{j\vartheta_2} \quad (34)$$

$$\boldsymbol{I}_1 = I_1 e^{j(\vartheta_1 - \varphi_1)} \quad (35)$$

$$\boldsymbol{I}_2 = I_2 e^{j(\vartheta_2 - \varphi_2)} \quad (36)$$

with

φ_1 input displacement angle

φ_2 output displacement angle.

All the amplitudes and the angles are time functions. Under balanced and sinusoidal steady state, all voltage and current amplitudes as well as φ_1, φ_2, are constant, whereas phase angles are linear functions of input and output angular frequencies with the form

$$\begin{aligned} \vartheta_1 &= \omega_1 t + \vartheta_{10} \\ \vartheta_2 &= \omega_2 t + \vartheta_{20}. \end{aligned} \quad (37)$$

Under the hypothesis of ideal converter behaviour regardless switching frequency, the averaged values of switching functions $\boldsymbol{H}_v$, $\boldsymbol{H}_i$, $\boldsymbol{S}_d$ and $\boldsymbol{S}_i$, are considered.

Concerning the IMC, the modulation is possible within inscribed circles to the hexagons of Fig. 4 and Fig. 5. Maximum values of $\boldsymbol{H}_v$ and $\boldsymbol{H}_i$ are limited to the radius of the circles. Hence (17) and (21) have to be multiplied by the ratio $\sqrt{3}/2$. Moreover considering (24) and (25), phase angles of $\boldsymbol{V}_2$ and of $\boldsymbol{I}_1$ are imposed by $\boldsymbol{H}_v$ and by $\boldsymbol{H}_i$ respectively. Therefore, taking into account (34), (35), the averaged values become

$$\boldsymbol{H}_v = \frac{1}{\sqrt{2}} m_v e^{j\vartheta_2} \quad (38)$$

$$\boldsymbol{H}_i = \sqrt{\frac{3}{2}} m_i e^{j(\vartheta_1 - \varphi_1)} \quad (39)$$

where $0 \le m_{v,i} \le 1$ are modulation factors.

By substitution of (38)-(39) and (33), (36) into (24)-(25), averaged relations (40) and (41) hold.

$$\boldsymbol{V}_2 = \frac{\sqrt{3}}{2} m V_1 e^{j\vartheta_2} cos\varphi_1 \quad (40)$$

$$\boldsymbol{I}_1 = \frac{\sqrt{3}}{2} m I_2 e^{j(\vartheta_1 - \varphi_1)} cos\varphi_2 \quad (41)$$

where $0 \le m = m_v, m_i \le 1$ is the total modulation factor.

By applying the maximum value $m = 1$, the well-known maximum voltage and maximum current transfer ratio under IMC approach can be obtained:

$$q_v = \frac{V_2}{V_1} = \frac{\sqrt{3}}{2} cos\varphi_1 \quad (42)$$

$$q_i = \frac{I_1}{I_2} = \frac{\sqrt{3}}{2} cos\varphi_2 \quad (43)$$

In general q_v and q_i are different each other because they depend by $cos\varphi_1$ and $cos\varphi_2$ respectively.

It must be evidenced that (42)-(43) are obtained by $\boldsymbol{H}_v$, $\boldsymbol{H}_i$ limited inside the inscribed circles of Fig. 4 and Fig. 5 respectively. Therefore, by admitting some degrees of over modulation, the limits (42)-(43), despite some distortion, can be overcome.

Furthermore, it must, also, be evidenced that voltage transfer ratio (42) has been derived by some authors [2], [9], [10] and [13] directly from MC in different ways. In this paper (42), (43) are deduced in a simple way from CSC and VSC relationships.

At this subject, it is interesting to recognize that Fig. 3, apparently similar to Figs. 4 and 5, does not allow to obtain similar gain limits from (5)-(6), because $\boldsymbol{s}_d$ and $\boldsymbol{s}_i$ are not independent of each other.

By applying (38), (39) into (29), (30) the $\boldsymbol{S}_d$ and $\boldsymbol{S}_i$, averaged over switching ripples, are obtained

$$\boldsymbol{S}_d = \frac{\sqrt{3}}{2} m e^{j(\vartheta_1+\vartheta_2-\varphi_1)} \tag{44}$$

$$\boldsymbol{S}_i = \frac{\sqrt{3}}{2} m e^{j(\vartheta_1-\vartheta_2-\varphi_1)}. \tag{45}$$

In (44), (45) only fixed states are used. More extensive expressions of $\boldsymbol{S}_d$ and $\boldsymbol{S}_i$ could be obtained using rotating states, but this aspect is out of the purpose of this paper.

6. Conclusion

The present paper has established and discussed the input-output space-vector relationships of MC and IMC. Thereafter the IMC approach has been compared with direct MC approach and direct MC basic equations are reconstructed from IMC ones.

The equivalence between IMC and the standard states of MC has been pointed out. IMC and MC are equivalent under the hypothesis that rotating configurations are not considered. With these hypothesis IMC has 36 fixed active configurations, among them 18 ones are different between each other and are the same of the MC's ones.

The maximum voltage and current ratios are straightforward deduced by IMC approach as product of CSC and VSC gains.

This paper clarifies that direct MC has in principle more switching states than IMC. In fact the so-called rotating states cannot be reproduced by IMC. In general many control strategies of MC use only 18 fixed configurations and hence, because the rotating states are claimed to be unnecessary to the control system by many authors, probably, full capability of MC cannot be employed. Indeed in [11] this fact is dealt with, in particular the maximum generation of input reactive power using all 27 switching configurations is analyzed.

As a consequence, control strategies that use all possible configurations should be analyzed and used to exploit full MC capabilities.

References

[1] P. Wheeler, J. Rodriguez, J. C. Clare, L. Empringham, and A. Weinstein, Matrix converter a technology review, *IEEE Trans. Ind. Electron*, 49, 276-288, 2002.

[2] J. W. Kolar, T. Friedli, J. Rodriguez, and P. W. Wheeler, Review of Three-Phase PWM AC–AC Converter Topologies, *IEEE Trans. Ind. Electron.*, 58, 4988-5006, 2011.

[3] J. Rodriguez, M. Rivera, J. W. Kolar, and P.W. Wheeler, A Review of Control and Modulation Methods for Matrix Converters, *IEEE Trans. Ind. Electron.*, 59, 58-70, 2012.

[4] S. Barcellona, M. S. Carmeli, and G. Superti-Furga, Comprehensive harmonic analysis of matrix converter under unbalanced/distorted conditions, *Electric Power System Research*, 96, 296-310, 2013.

[5] J. W. Kolar, F. Schafmeister, S. D. Round, and H. Ertl, Novel Three-Phase AC–AC Sparse Matrix Converters, *IEEE Trans. Power Electron.*, 22, 1649-1661, 2007.

[6] F. Gruson, P. Le Mogne, P. Delarue, M. Arpillière, and X. Cimetiere, Comparison of Losses between Matrix and Indirect Matrix Converters with an Improved Modulation, *IEEE International Symposium Ind. Electron.* (2010) 718-723.

[7] N. Taib, B. Metidji, and T. Rekioua, Performance and efficiency control enhancement of wind power generation system based on DFIG using three-level sparse matrix converter, *International Journal of Electrical Power and Energy Systems* (2013), 53 (1), 287-296.

[8] D. Casadei, G. Serra, and A. Tani, A general approach for the analysis of the input power quality in matrix converters, *IEEE Trans. Power Electron.*, 13, 882-891, 1998.

[9] D. Casadei, G. Serra, A. Tani, and L. Zarri, Matrix Converter Modulation Strategies: A New General Approach Based on Space-Vector Representation of the Switch State, *IEEE Trans. Ind. Electron.* 49, 370-381, 2002.

[10] J. W. Kolar, T. Friedli, F. Krismer, and S. D. Round, The Essence of Three-Phase ACAC Converter Systems, *Power Electron. and Motion Conference*, 27-42, 2008.

[11] H. Hojabri, H. Mokhtari, and Liuchen Chang, A Generalized Technique of Modeling, Analysis, and Control of a Matrix Converter Using SVD, *IEEE Trans. Ind. Electron.*, 58 (2011) 949-959.

[12] A. Alesina and M. G. B. Venturini, Solid-state power conversion: A Fourier analysis approach to generalized transformer synthesis, *IEEE Trans. Circuits Syst.*, CAS-28, 319-330, 1981.

[13] A. Alesina and M. G. B. Venturini, Analysis and design of optimum amplitude nine-switch direct AC–AC converters, *IEEE Trans. Power Electron.*, 4, 101-112, 1989.

[14] L. Huber and D. Borojevic, Space vector modulated three-phase to three-phase matrix converter with input power factor correction, *IEEE Trans. Ind. Appl.*, 31,1234-1246, 1995.

[15] C. Ponmani, and M. Rajaram, Compensation strategy of matrix converter fed induction motor drive under input voltage and load disturbances using internal model control, *International Journal of Electrical Power and Energy Systems*, 44 (1), 43-51, 2013.

[16] A. Arias, C. Ortega, J. Zaragoza, J. Espina, and J. Pou, Hybrid sensorless permanent magnet synchronous machine four quadrant drive based on direct matrix converter, *International Journal of Electrical Power and Energy Systems*, 45 (1), 78-86, 2013.

[17] Xiao Wang, and K. J. Tseng, Novel space vector based hysteresis current control (HCC) strategies for matrix converter, in EPE, *European Conference on Power Electronics and Applications*, 1-10, 2005.

[18] Shuyun Jia, and K. J. Tseng, A rule-based control strategy for matrix converters, in *Proc. 21st IEEE APEC '06*, 1490-1495, 2006.

[19] A. K. Rao, J. K. Chatterjee, S. Subramanian, and V. Rajasekhar, Improved Operation of a Three Phase Matrix Converter using simple modulation strategy, *Power Electron., Drives and Energy System (PEDES) & 2010 Power India*, Joint Int. Conf., 1-8, 2010.

[20] S. Lekhchine, T. Bahi, Y. Soufi, and S. Lachtar, Modeling and performance study of indirect matrix converter fed induction motor, *Journal of Electrical Systems*, 8 (4), 411-424, 2012.